OPEN ACCESS Freely available online

PLoS one

Characterization of Multiple Ion Channels in Cultured Human Cardiac Fibroblasts

Gui-Rong Li[1,2]*, Hai-Ying Sun[1], Jing-Bo Chen[1], Yuan Zhou[1,2], Hung-Fat Tse[1], Chu-Pak Lau[1]

1 Department of Medicine and Research Centre of Heart, Brain, Hormone and Healthy Aging, Li Ka Shing Faculty of Medicine, The University of Hong Kong, Pokfulam, Hong Kong Special Administrative Region (SAR), China, **2** Department of Physiology, Li Ka Shing Faculty of Medicine, The University of Hong Kong, Pokfulam, Hong Kong Special Administrative Region (SAR), China

Abstract

Background: Although fibroblast-to-myocyte electrical coupling is experimentally suggested, electrophysiology of cardiac fibroblasts is not as well established as contractile cardiac myocytes. The present study was therefore designed to characterize ion channels in cultured human cardiac fibroblasts.

Methods and Findings: A whole-cell patch voltage clamp technique and RT-PCR were employed to determine ion channels expression and their molecular identities. We found that multiple ion channels were heterogeneously expressed in human cardiac fibroblasts. These include a big conductance Ca^{2+}-activated K^+ current (BK_{Ca}) in most (88%) human cardiac fibroblasts, a delayed rectifier K^+ current (IK_{DR}) and a transient outward K^+ current (I_{to}) in a small population (15 and 14%, respectively) of cells, an inwardly-rectifying K^+ current (I_{Kir}) in 24% of cells, and a chloride current (I_{Cl}) in 7% of cells under isotonic conditions. In addition, two types of voltage-gated Na^+ currents (I_{Na}) with distinct properties were present in most (61%) human cardiac fibroblasts. One was a slowly inactivated current with a persistent component, sensitive to tetrodotoxin (TTX) inhibition ($I_{Na.TTX}$, $IC_{50} = 7.8$ nM), the other was a rapidly inactivated current, relatively resistant to TTX ($I_{Na.TTXR}$, $IC_{50} = 1.8$ μM). RT-PCR revealed the molecular identities (mRNAs) of these ion channels in human cardiac fibroblasts, including KCa.1.1 (responsible for BK_{Ca}), Kv1.5, Kv1.6 (responsible for IK_{DR}), Kv4.2, Kv4.3 (responsible for I_{to}), Kir2.1, Kir2.3 (for I_{Kir}), Clnc3 (for I_{Cl}), $Na_V1.2$, $Na_V1.3$, $Na_V1.6$, $Na_V1.7$ (for $I_{Na.TTX}$), and $Na_V1.5$ (for $I_{Na.TTXR}$).

Conclusions: These results provide the first information that multiple ion channels are present in cultured human cardiac fibroblasts, and suggest the potential contribution of these ion channels to fibroblast-myocytes electrical coupling.

Citation: Li G-R, Sun H-Y, Chen J-B, Zhou Y, Tse H-F, et al. (2009) Characterization of Multiple Ion Channels in Cultured Human Cardiac Fibroblasts. PLoS ONE 4(10): e7307. doi:10.1371/journal.pone.0007307

Editor: Alicia J. Kowaltowski, Instituto de Química, Universidade de São Paulo, Brazil

Received May 18, 2009; **Accepted** September 14, 2009; **Published** October 6, 2009

Funding: This study was supported by a General Research Fund (HKU 7603/06M) from Research Grant Council of Hong Kong. The funder had no role in study design, data collection and analysis, decision to publish, or preparation of the manuscript.

Competing Interests: The authors have declared that no competing interests exist.

* E-mail: grli@hkucc.hku.hk

Introduction

It is generally recognized that cardiac myocytes and fibroblasts form extensive networks in the heart, with numerous anatomical contacts between cells [1]. Cardiac fibroblasts play a central role in the maintenance of extra-cellular matrix in the normal heart and act as mediators of inflammatory and fibrotic myocardial remodeling in the injured heart, e.g. ischemic, hypertensive, hypertrophic, and dilated cardiomyopathies, and heart failure [2,3]. The cardiac myocyte network, coupled with gap junctions, is generally believed to be electrically isolated from fibroblasts in vivo. However, in the co-culture of cardiac myocytes and fibroblasts, the heterogeneous cell types form functional gap junctions, providing a substrate for electrical coupling of distant myocytes, interconnected by fibroblasts. In addition to the evidence of fibroblast-to-myocyte electrical coupling in the rabbit SA node [4], fibroblasts have been shown to be coupled electrotonically with myocytes in vitro [1,5–8]. Moreover, there is increasing evidence that implicates potential heterocellular electrical coupling in the diseased myocardium with arrhythmogenesis [9,10]; therefore, the cardiac fibroblasts are considered to be potential targets in managing cardiac disorders including hypertrophy, heart failure and arrhythmias [2,3,9,10].

Ion channels and their functions are well studied in cardiomyocytes; however, the ion channel expression and their physiological roles are not fully understood in cardiac fibroblasts. An inward rectifier K^+ current (I_{Kir}), a delayed rectifier K^+ current (IK_{DR}), and a non-selective cation channel current were recently reported in rat ventricular fibroblasts [11–13]. Although a Ca^{2+}-activated big conductance K^+ current (BK_{Ca}) was described in human cardiac fibroblasts [14], it is unknown whether other types of ion channel currents are present in human cardiac fibroblasts. The present study was designed to employ the approaches of whole-cell patch voltage clamp and RT-PCR to examine the functional ion channels in human cardiac fibroblasts. Using these techniques, we identified multiple ion channels expressed in cultured human cardiac fibroblasts.

Methods

Cell cultures

Human cardiac fibroblasts (adult ventrical, Catalog# 6310) were purchased from ScienCell Research Laboratory (San Diego,

CA). The cells were cultured as monolayers in completed DMEM containing 10% fetal bovine serum (Invitrogen, Hong Kong) and antibiotics (100 U/ml penicillin G and 100 μg/ml streptomycin) at 37°C in a humidified atmosphere of 95% air, 5% CO_2. No difference in cell growth and ion channel expression were observed with either our culture medium or the medium from ScienCell Research Laboratory. Cells used in this study were from the early passages 2 to 6 to limit the possible variations in functional ion channel currents and gene expression. The cells were harvested for electrophysiological recording and RT-PCR determination via trypsinization [15].

Solutions and reagents

Tyrode solution for electrophysiological study contained (mM): 140 NaCl, 5.0 KCl, 1.0 $MgCl_2$, 1.8 $CaCl_2$, 10 glucose, and 10 HEPES; pH was adjusted to 7.3 with NaOH. The standard pipette solution contained (mM): 20 KCl, 110 K-aspartate, 1.0 $MgCl_2$, 10 HEPES, 0.05 EGTA, 0.1 GTP, 5.0 Na_2-phosphocreatine, and 5.0 Mg-ATP; pH was adjusted to 7.2 with KOH. When Na^+ current was determined, K^+ in pipette and bath solutions was replaced by equimolar Cs.

For volume sensitive chloride current ($I_{Cl.vol}$) recording, hypotonic 0.7T (~210 mosmol/L) Tyrode solution was made by reducing NaCl from 140 to 98 mM. When 1.0T (~300 mosomol/L) solution was prepared, 90 mM mannitol was added. The pipette solution for recording $I_{Cl.vol}$ contained (mM) 110 CsCl, 20 Cs-aspartate, 5 EGTA, 1.0 $MgCl_2$, 10 HEPES, 0.1 GTP, 5.0 Na_2-phosphocreatine, and 5.0 Mg-ATP (pH = 7.2 with CsOH).

The chloride channel blocker 5-nitro-1-(3-phenylpropylamino) benzoic acid (NPPB) was purchased from Tocris (Bristol, UK). All the other chemicals including DIDS (4,4′-diisothiocyanostilbene-2,2′-disulfonic acid) were purchased from Sigma-Aldrich (St Louis, MO).

Electrophysiology

A small aliquot of the solution containing the cardiac fibroblasts was placed in an open perfusion chamber (1 ml) mounted on the stage of an inverted microscope. The cells were allowed to adhere to the bottom of the chamber for 10–20 min, and then superfused at 2–3 ml/min with Tyrode solution. The studies were conducted at room temperature (22–24°C).

The membrane ionic currents were recorded with a whole-cell patch-clamp technique as described previously [16]. Borosilicate glass electrodes (1.2 mm OD) were pulled with a Brown–Flaming puller (Model P-97, Sutter Instrument Co. Novato, CA), and had tip resistances of 2~3 MΩ when filled with pipette solution. The tip potentials were compensated before the pipette touched the cell. After a gigaohm-seal was obtained by negative pressure suction, the cell membrane was ruptured by a gentle suction to establish whole-cell configuration with a seal resistance >800 MΩ. The cell membrane capacitance (49.6±12.1 pF) was electrically compensated with the Pulse software. The series resistance (R_s, 3–5 MΩ) was compensated by 50–70% to minimize voltage errors. Membrane currents were elicited with voltage protocols as described in the following Results section for individual different current recording. Data were acquired with an EPC10 amplifier (Heka, Lambrecht, Germany). The membrane currents were low-pass filtered at 5 kHz and stored on the hard disk of an IBM compatible computer.

Messenger RNA determination

The messenger RNA was examined using RT-PCR technique using Table 1 primers as described previously [15]. Total RNA was extracted from human cardiac fibroblasts using Trizol reagent (Invitrogen), and further treated with DNase I (GE Healthcare, Hong Kong) for 30 min at 37°C, then heated to 75°C for 5 min and finally cooled to 4°C [17]. Reverse transcription was performed using a RT system (Promega, Madison, WI) in a 20 μl reaction mixture. A total of 2 μg RNA was used in the reaction and a random hexamer primer was used for the initiation of cDNA synthesis. After the RT procedure, the reaction mixture (cDNA) was used for PCR.

PCR was performed with thermal cycling conditions of 94°C for 2 min followed by 35 cycles at 94°C for 45 s, 55–58°C for 45 s, and 72°C for 1 min using a Promega PCR kit and oligonucleotide primers as shown in Table 1. This was followed by a final extension at 72°C (10 min) to ensure complete product extension. The PCR products were electrophoresed through 1.5% agarose gels and visualized under a UV transilluminator (BioRad, Hercules, CA) after staining with ethidium bromide.

Statistical analysis

Results are presented as means ± SEM. Paired and/or unpaired Student's *t*-tests were used as appropriate to evaluate the statistical significance of differences between two group means, and analysis of variance was used for multiple groups. Values of $P<0.05$ were considered to indicate statistical significance.

Results

Families of membrane ionic currents in human cardiac fibroblasts

Figure 1 illustrates the families of membrane currents recorded in human cardiac fibroblasts using a standard pipette solution. Five types of membrane currents were observed in human cardiac fibroblasts (in a total of 265 cells). One current was activated at depolarization voltages between −70 and +60 from a holding potential of −80 mV (0.2 Hz), and showed an outward current with noisy oscillation between +20 and +60 mV (Fig. 1A). These features suggest that this current is likely a big conductance Ca^{2+}-activated K^+ current (BK_{Ca}) [15]. The noisy oscillatory BK_{Ca} was present with other currents in most (88%, 233 of 265) of fibroblasts. Another current activated by the same protocol was a transient outward current (Fig. 1B), and presented in 15% (40 of 265) of cells. Third current was an inward component activated by hyperpolarization voltage steps a holding potential of −40 mV and co-existed with the noisy oscillatory current activated by depolarization voltage steps. This inward component exhibited the properties similar to inward rectifier K^+ current (I_{Kir}) (Fig. 1C). I_{Kir} was observed in 24% (64 of 265) of cells. Fourth current was elicited by voltage steps between −120 and +60 from a holding potential of −40 mV, showing a very small inward component and a large outward current with outward rectification (Fig. 1D). This current was observed in 7% (19 of 265) of cells. Moreover, an inward current coexists with the oscillatory current in 61% (167 of 265) of human cardiac fibroblasts (Fig. 1E and 1F). Interestingly, the inward current exhibits either a fast inactivation (Fig. 1E) or a slow (Fig. 1F) inactivation.

Ca^{2+}-activated noisy oscillatory current

Figure 2A displays the noisy oscillatory BK_{Ca} reversibly suppressed by the BK_{Ca} blocker paxilline (1 μM, 5 min exposure) in a representative fibroblast. Current-voltage (*I-V*) curves recorded with a 2-s voltage ramp (−80 to +80 mV from a holding potential of −40 mV) in the absence of paxilline showed outward rectification (control) in another cell. The outwardly-rectifying current was remarkably reduced by paxilline (Fig. 2B). The current at +60 mV was reduced from 29.8±5.3 pA/pF of control

Table 1. Human gene specific-primers for RT-PCR.

Gene name	Accession No.	Forward primer(5′–3′)	Reverse primer (5′–3′)	Product size (bp)
GAPDH	J02642	AACAGCGACACCCACTCCTC	GGAGGGGAGATTCAGTGTGGT	258
KCa1.1	U11058	ACAACATCTCCCCCAACC	TCATCACCTTCTTTCCAATTC	310
KCa3.1	NM_002250	TGAGACGCCGAAAGCG	GCAGAGGAGTAAGAAGGTGGAA	187
KCa2.1	NM_170782	GAAGTTCCTCCAAGCTATCCA	TCTTTCCGTTCCCTGGTCT	498
Kv1.4	NM_002233	CCAGAGGAACCAGGAGTC	CCACAGATAGAGGCAAAGA	426
Kv1.5	NM_002234	CAGTTCCCCAACACACTCCT	CTGAACTCAGGCAGGGTCTC	410
Kv1.6	NM_002235	CCTGTCGCTGTTTCCG	ACCACCATTGTTTCCACC	456
Kv2.1	NM_004975	GAGCAGATGAACGAGGAGC	ACAGGGCAATGGTGGAGA	196
Kv3.1	NM_004976	CGAGGACGAGCTGGAGATG	CCTTGGCTGCCTTGGAG	479
Kv4.2	NM_012281	ACATGCAGAGCAAACGGAA	GGACTGTGACTTGAAGGACGA	220
Kv4.3	AF187963	GCCTCCGAACTAGGCTTTCT	CCCTGCGTTTATCAGCTCTC	310
Kir1.1	NM_153765	GGGACTTGCTCACATCG	CCACATTGCCAAATTCTAT	355
Kir2.1	NM_000891	ACTTCCACTCCATGTCCC	CTTTACTCTTCCCGTTCC	365
Kir2.2	BC027982	CCAAGAAGCGGGCACAGA	TGGGCGACACCAGAAAGAT	243
Kir2.3	NM_152868	CGGAGACCCCAAGACCCA	TGCTCAGGTTGGCGAAGT	340
Clcn2	NM_004366	AAGCGTGTCCGAATCTCC	ACCTCAGTGGTCTCCGTGT	368
Clcn3	NM_173872	CATAGGTCAAGCAGAGGGTC	TATTTCCGCAGCAACAGG	293
Nav1.1	NM_006920	GAGAACGACTTCGCAGATG	CACCAACCAAGGAAACCA	208
Nav1.2	NM_021007	CCCCTTCTACCCTCACATCT	ACACTGCTGAACTGCTCC	394
Nav1.3	NM_006922	AAAGAGCCGTGAGCATAG	ATCCCTCCACATTTGACA	432
Nav1.4	NM_000334	GTCATTCGCACCATCCTA	TCTCGCACTCAGACTTGTT	454
Nav1.5	NM_198056	ATGGACCCGTTTACTGACC	CCACTGAGTTCCCGATGAT	367
Nav1.6	NM_014191	TGCGGGAAAGTACCACTA	AGAAGGAGCCGAAGATGA	314
Nav1.7	NM_002977	AAAAGGCGTTGTAGTTCC	CAGTCATTGGGTGGTGTT	310
Nav1.8	NM_006514	AACTTCCGTCGCTTTACTC	GAAGGTCAGTTCGGGTCA	424
Nav1.9	NM_006514	TGATGACTGACCCGTTTA	ACAATGACCAGGACCACA	415

GAPDH, glyceraldehyde-3-phosphate dehydrogenase; KCa, Ca^{2+}-activated K^+ channel; Kv, voltage-gated K^+ channel; Kir, inward rectifier K^+ channel; Clcn Cl^- channel; Nav, voltage-gated Na^+ channel.

doi:10.1371/journal.pone.0007307.t001

to 3.9±2.1 pA/pF with 1 μM paxilline (n = 35, P<0.01 vs control).

We found that a paxilline-resistant current was present in a small population of human cardiac fibroblasts (14.2%, 5 of 35 cells). Figure 2C displays that paxilline (1 μM) partially suppressed the membrane current (+60 mV, to 8.9±1.6 pA/pF from 21.8.1±2.9, P<0.01); the remaining current was inhibited by 5 mM 4-aminopyridine (4-AP, to 2.1±1.1 pA/pF, n = 5, P<0.01) (Fig. 2C). This suggests that a 4-AP sensitive delayed rectifier K^+ current (IK_{DR}) is co-present with BK_{Ca} in these cells.

Transient outward K^+ current

The transient outward K^+ current I_{to} was present in 15% of cardiac fibroblasts. I_{to} in human cardiac myocytes was sensitive to inhibition by 4-AP [18], therefore we determined whether I_{to} in human fibroblasts could be decreased by 4-AP. Figure 3A shows the I_{to} traces recorded in a typical experiment in the absence and presence of 5 mM 4-AP. I_{to} (+60 mV) was substantially inhibited by 4-AP to 11.9±1.4 pA/pF from 36.5±2.6 pA/pF (n = 7, P<0.01).

Figure 3B illustrates the mean values of voltage-dependent activation (g/g_{max}) and inactivation (availability, I/I_{max}) of I_{to}. The g/g_{max} was determined from the *I-V* relationship of each cell as previously described [19]. The I/I_{max} was determined with the protocol as shown in the left *inset* (with 1-s conditioning pulses from voltages between −100 and −10 mV followed by a 300-ms test pulse to +60 mV). Data were fitted to a Boltzmann distribution to obtain the half activation or availability voltage ($V_{0.5}$) and the slope factor (S). The $V_{0.5}$s of activation and availability of I_{to} were 11.2±0.4 mV (n = 7) and −40.6±1.5 mV (n = 9), and the S was 11.1±1.1 and −8.4±1.3, respectively.

Fig. 3C shows the time course of the mean values of I_{to} recovery from inactivation, determined with a paired-pulse protocol as shown in the *inset*. I_{to} recovery was complete within 900 ms and fitted to a mono-exponential function with time constant (τ) of 257.4±5.9 ms (n = 7). These properties of I_{to} in human cardiac fibroblasts, i.e. 4-AP sensitivity, voltage-dependent activation and availability, and recovery from inactivation, are similar to those observed in human cardiac myocytes [19] and mesenchymal stem cells [15], though there are differences in the values of the recovery time constant and the $V_{0.5}$s of voltage-dependent activation and availability.

Inward rectifier K^+ current

It is generally believed that inwardly-rectifying K^+ channels are sensitive to inhibition by Ba^{2+} [20], therefore we determined the

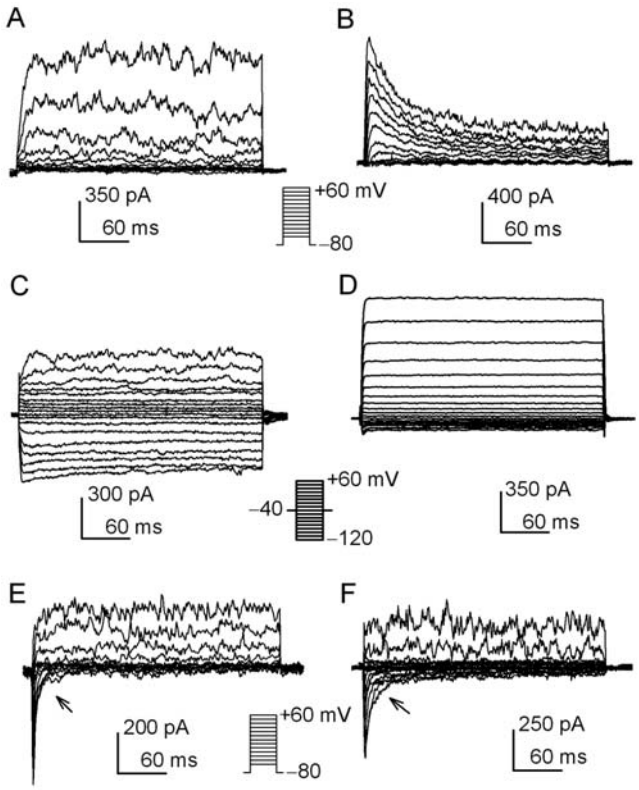

Figure 1. Families of membrane currents in human cardiac fibroblasts. ***A.*** Noisy current was activated at positive potential. Currents were elicited with the protocol shown in the *inset* (0.2 Hz). ***B.*** A transient outward current was activated in a human cardiac fibroblast by the same protocol as in A. ***C.*** A current with inward rectification activated by hyperpolarized potentials (*inset*) was co-present with the noisy current. ***D.*** Voltage-dependent current with outward rectification was recorded with the same protocol as in C. ***E.*** An inward current with fast inactivation activated by depolarization voltage steps (*inset*) was co-present with the noisy current. ***F.*** An inward current with slow inactivation (arrow) activated by the same protocol as in E was co-present with the noisy current.
doi:10.1371/journal.pone.0007307.g001

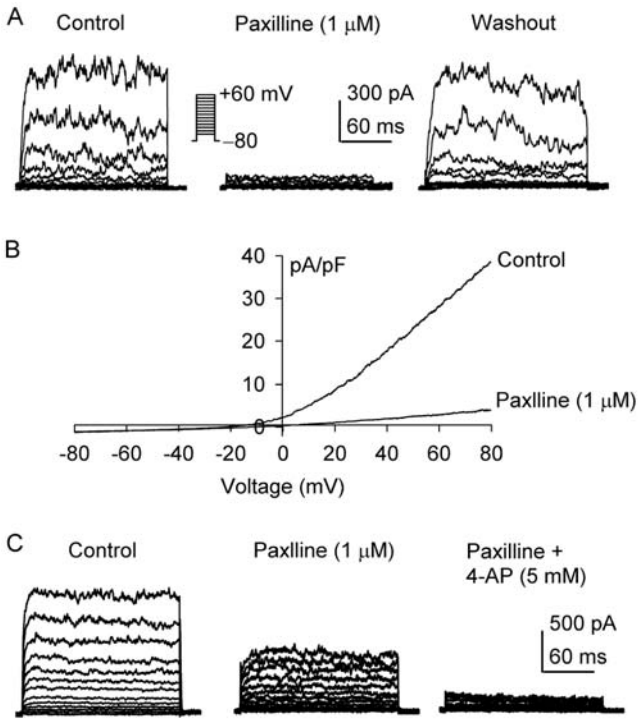

Figure 2. BK_{Ca} and IK_{DR} in human cardiac fibroblasts. ***A.*** Voltage-dependent current was reversibly suppressed by the BK_{Ca} blocker paxilline (1 μM). Currents were elicited by the voltage protocol as shown in the *inset*. ***B.*** Current-voltage (*I-V*) relationships of membrane current were recorded by a 2-s ramp protocol (−80 to +80 mV from a holding potential −40 mV) in a representative cell in the absence and presence of 1 μM paxilline. ***C.*** Membrane currents recorded in a typical experiment with the same voltage protocol as in A were partially inhibited by 1 μM paxilline. The remaining current was suppressed by co-application of paxilline and 5 mM 4-AP.
doi:10.1371/journal.pone.0007307.g002

effect of Ba^{2+} on I_{Kir} in human cardiac fibroblasts. Figure 4 shows the current traces recorded in a representative cell with the voltage protocol as shown in the *inset* in the absence (control) and presence of Ba^{2+}. Ba^{2+} (0.5 mM) reversibly reduced I_{Kir}. Figure 4B displays that the increase of external K^+ (K^+_o, from 5 to 20 mM) enhanced I_{Kir} conductance. Basal I_{Kir} and the high K^+_o-induced current were suppressed by Ba^{2+}. Figure 4C illustrates the *I-V* relationships of I_{Kir} recorded in a representative cell with a 2-s ramp protocol (−120 to 0 mV from −40 mV) in solution containing 5 mM K^+ (control) or 20 mM K^+, and after application of 0.5 mM Ba^{2+} in bath solution. Ba^{2+} strongly inhibited I_{Kir}. Ba^{2+}-sensitive current was obtained by digitally subtracting currents before and after application of Ba^{2+} (Fig. 4D). The *I-V* relationships of Ba^{2+}-sensitive I_{Kir} in 5 and 20 mM K^+_o exhibited a strong inward rectification, typical of an inwardly-rectifying K^+ current. Similar results were obtained in 5 other cells.

Volume-sensitive chloride current in human cardiac fibroblasts

The current with outward rectification shown in Fig. 1D was insensitive to inhibition of K^+ channel blockers including 5 mM tetraethylammonium (TEA), 5 mM 4-AP, or 0.5 mM Ba^{2+} (n = 4−6), suggesting that the outwardly-rectifying current is not carried by K^+ ion. We then employed the Cl^- channel inhibitor DIDS to determine whether the current is carried by chloride ions. Figure 5A shows the current traces recorded in a representative cell with the protocol shown in the *inset*; DIDS (150 μM) suppressed the current. The *I-V* relationship (Fig. 5B) of the DIDS-sensitive current obtained by subtracting control currents by the current recorded after DIDS application displayed outward rectification and had a reversal potential at −35 mV, which is close to Cl^- equilibrium potential (E_{Cl}, −46.8 mV). Similar results were obtained in a total of 6 cells. This result suggests that the recorded current under isotonic conditions is carried by Cl^- ions.

To investigate whether the Cl^- channel is volume sensitive in human cardiac fibroblasts, we employed a 0.7T tonic solution and recorded membrane current using a K^+-free pipette solution, symmetrical Cl^- ion in pipette and bath medium as described in the Methods section. The membrane conductance was remarkably enhanced by exposure to 0.7T (20 min), and the increased current was highly suppressed by the Cl^- channel blocker NPPB (Fig. 5C). The *I-V* relationship of 0.7T-induced Cl^- current is linear under symmetrical Cl^- conditions Fig. 5D), similar to the previous report [21]. These results indicate that volume-sensitive Cl^- channel ($I_{Cl,vol}$) is present in human cardiac fibroblasts.

Inward Na^+ currents in human cardiac fibroblasts

The depolarization-elicited inward currents (Fig. 1E and 1F) were studied under K^+-free conditions. Figure 6 illustrates two types of

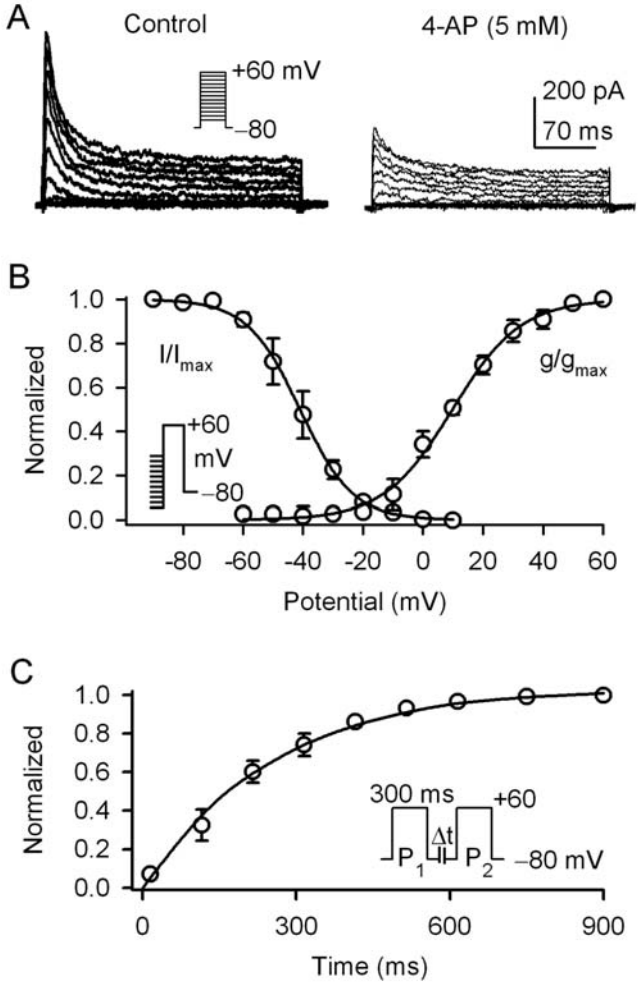

Figure 3. I_{to} in human cardiac fibroblasts. ***A.*** I_{to} traces recorded in a representative cell with the voltage protocol showed in the *inset* in the absence and presence of 5 mM 4-AP. ***B.*** Normalized mean values of voltage-dependent availability (I/I_{max}) and activation conductance (g/g_{max}) of I_{to} were fitted to the Boltzmann function: $y = 1/\{1+\exp[(V_m-V_{0.5})/S]\}$, where V_m is membrane potential, $V_{0.5}$ is the estimated midpoint, and S is the slope factor. ***C.*** Normalized I_{to} (I_2/I_1) plotted vs. P_1-P_2 interval. The recovery curve was fitted to a mono-exponential function. The I_{to} was measured from the current peak to the 'quasi'-steady-state level.
doi:10.1371/journal.pone.0007307.g003

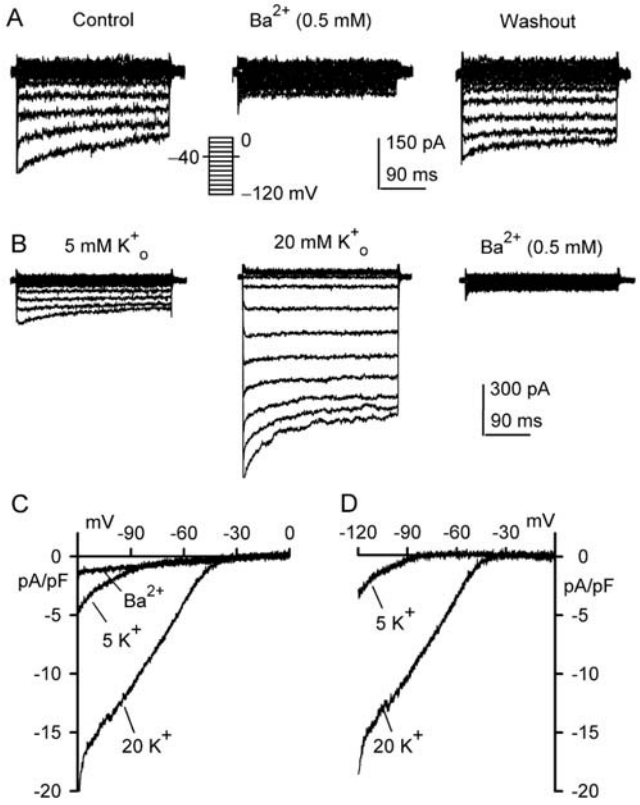

Figure 4. Effect of Ba^{2+} on membrane current in human cardiac fibroblasts. ***A.*** Voltage-dependent currents were reversibly inhibited by 0.5 mM $BaCl_2$ in a representative cell. Currents were recorded with the protocol as shown in the *inset* (0.2 Hz). ***B.*** Voltage-dependent current recorded in another cell with voltage protocol shown in the *inset* of A was increased by elevating K^+_o from 5 to 20 mM. Ba^{2+} (0.5 mM) remarkably suppressed the current. ***C.*** Left panel: *I-V* relationships of membrane currents recorded in a representative cell with a 2-s ramp protocol (−120 to 0 mV from a holding potential of −40 mV) in 5 mM K^+_o, 20 mM K^+_o, and after application of 0.5 mM Ba^{2+}. Right panel: Ba^{2+}-sensitive *I-V* relationships of the membrane current, typical of I_{Kir}.
doi:10.1371/journal.pone.0007307.g004

inward currents recorded in human cardiac fibroblasts with voltage steps (50 ms) to between −60 and +70 mV from −80 mV (*inset*) in 10-mV increments at 0.2 Hz. One of these currents exhibited an incomplete inactivation (or a persistent component) during 50 ms depolarization (control of Fig. 6A, 6B), similar to L-type Ca^{2+} current ($I_{Ca.L}$) in human cardiac myocytes [22]. However, this current was insensitive to inhibition by a high concentration of the $I_{Ca.L}$ blocker nifedipine (10 μM), in contrast with human cardiac $I_{Ca.L}$, which is fully suppressed by nifedipine [22]. Interestingly, the current was abolished by replacing bath Na^+ (Na^+_o) with equimolar choline, and recovered upon restoration of Na^+_o (Fig. 6A, n = 6). In addition, this current is sensitive to inhibition by 10 and 100 nM tetrodotoxin (TTX), and the effect was reversed by washout (n = 6). These results suggest that this inward current is likely a TTX-sensitive I_{Na} ($I_{Na.TTX}$) with a persistent component.

Another inward current exhibited a complete inactivation (control of Fig. 6C & 6D). This current had no response to 10 nM TTX; however, nifedipine (10 μM) reversibly reduced the current (Fig. 6C, n = 7). Replacement of Na^+_o with equimolar choline reversibly abolished this inward current, and the current required a high concentration (10 μM) of TTX for a substantial suppression (Fig. 6D, n = 6). These results suggest that this inward current is likely a TTX-resistant Na^+ current ($I_{Na.TTXR}$).

The concentration-dependent inhibitory effects of TTX on $I_{Na.TTX}$ and $I_{Na.TTXR}$ at 0 mV are illustrated in Fig. 6E. The IC_{50} (50% inhibitory concentration) of TTX for inhibiting $I_{Na.TTX}$ was 7.8 nM with a coefficient of 0.94, while the IC_{50} of TTX for inhibiting $I_{Na.TTXR}$ was 1.8 μM with a Hill coefficient of 0.58. The $I_{Ca.L}$ blocker nifedipine had no significant inhibitory effect on $I_{Na.TTX}$, whereas it inhibited $I_{Na.TTXR}$ with an IC_{50} of 56.2 μM and a Hill coefficient of 0.59 (Fig. 6F).

The *I-V* relationships for the peak current of $I_{Na.TTX}$ and $I_{Na.TTXR}$ are illustrated in Fig. 7A. $I_{Na.TTX}$ had a threshold potential of −40 mV and peaked at +10 mV, while $I_{Na.TTXR}$ had a threshold potential of −50 mV and peaked at 0 mV. Inactivation of $I_{Na.TTX}$ and $I_{Na.TTXR}$ was fitted to a monoexponential function with time constant (τ) as shown in the left panel of Fig. 7B. The inactivation process of $I_{Na.TTX}$ was slower than that of $I_{Na.TTXR}$ (Fig. 7B, n = 12, $P<0.01$ at −20 to +60 mV).

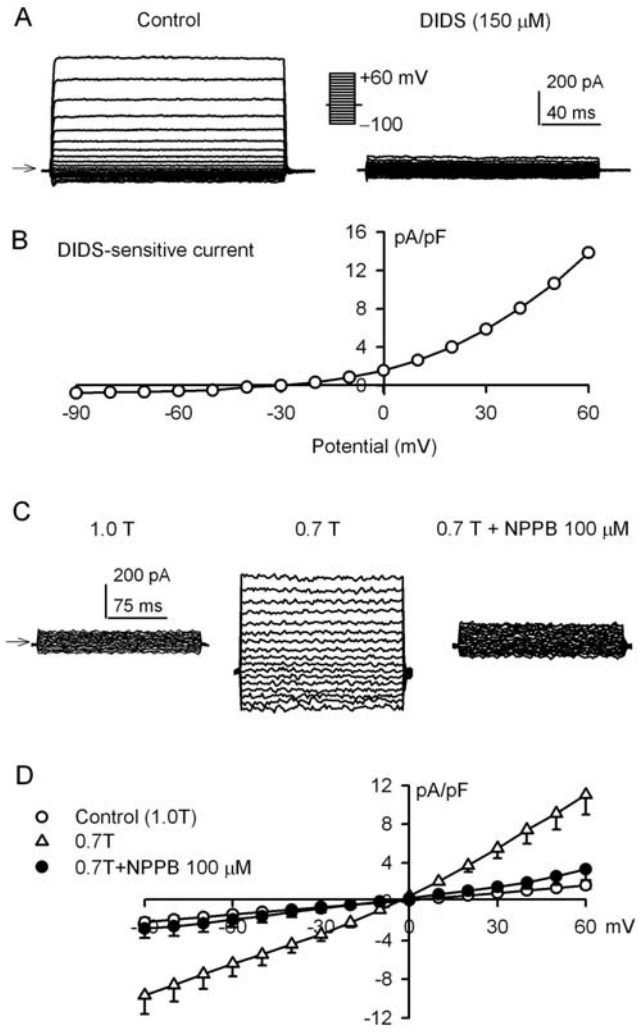

Figure 5. I_{Cl} in human cardiac fibroblasts. A. Voltage-dependent current was inhibited by the Cl^- channel blocker DIDS (150 μM). Current was elicited by the voltage steps as shown in the *inset* (0.2 Hz). ***B.*** *I-V* relation curve of DIDS-sensitive current obtained by subtracting currents before and after DIDS application in A. ***C.*** Voltage-dependent current recorded in a representative cells during control, after 20 min 0.7T exposure and application of 100 μM NPPB. ***D.*** *I-V* relationships for control current (1.0T), 0.7T and 0.7T with 100 μM NPPB. The 0.7T-induced current was significantly inhibited by NPPB at all test potentials (n = 5, P<0.01). The arrows in the figure indicate the zero current level.
doi:10.1371/journal.pone.0007307.g005

Figure 7C illustrates the mean values of the steady-state voltage dependent activation (g/g_{max}) and inactivation (availability, I/I_{max}) for both $I_{Na.TTX}$ and $I_{Na.TTXR}$. The g/g_{max} was determined from the *I-V* relationships of each cell in Fig. 7A as previously described [23]. The I/I_{max} was determined with the protocol as shown in the left *inset* (with 1-s conditioning pulses from voltages between −120 and −10 mV then to a 50-ms test pulse to 0 mV). Data were fitted to a Boltzmann equation. The $V_{0.5}$s of g/g_{max} and I/I_{max} for $I_{Na.TTX}$ were −7.2±1.1 mV (n = 9) and −61.4±1.6 mV (n = 10), and the S was 8.7±1.2 and −10.8±1.2, respectively. While the $V_{0.5}$s of g/g_{max} and I/I_{max} for $I_{Na.TTXR}$ were −24.7±1.4 (n = 7) and −72.3±1.5 (n = 9) mV, and the S was 7.5±1.1 and −8.5±1.3, respectively. The $V_{0.5}$s of g/g_{max} and I/I_{max} were more positive in $I_{Na.TTX}$ than those in $I_{Na.TTXR}$ (P<0.01).

Figure 7E shows the time course of mean values of recovery of $I_{Na.TTX}$ or $I_{Na.TTXR}$ from inactivation, which was determined using a paired-pulse protocol shown in the *inset* as described previously [23]. The recovery of $I_{Na.TTX}$ and $I_{Na.TTXR}$ from inactivation was complete within 150 ms, and the curves were fitted to a mono-exponential function. The time constant (τ) was 14.3±2.1 ms for $I_{Na.TTX}$ (n = 11) and 21.4±2.9 ms for $I_{Na.TTXR}$ (n = 9). The recovery of $I_{Na.TTXR}$ from inactivation was slower than that of $I_{Na.TTX}$ (P<0.05). These results indicate that two types of Na^+ channels with distinct TTX-sensitivity and kinetics are present in human cardiac fibroblasts.

Messenger RNAs of functional ion channels

To explore the molecular identities of the functional ionic currents, we examined gene expression of various ionic channels in human cardiac fibroblasts with RT-PCR using the specific primers targeting human genes for KCa, Kv, Kir, Clcn, and Na_V channel families as shown in Table 1. Figure 8A displays the significant gene expression of KCa1.1 (responsible for BK_{Ca}), Kv1.5, Kv1.6 (responsible for IK_{DR}), Kv4.2, Kv4.3 (responsible for I_{to}), Kir2.1, Kir2.3 (for I_{Kir}), Clcn3 (for $I_{Cl.vol}$), $Na_V1.2$, $Na_V1.3$, $Na_V1.6$ and $Na_V1.7$ (for $I_{Na.TTX}$), and $Na_V1.5$ (for $I_{Na.TTXR}$) in human cardiac fibroblasts. In addition, Clcn2 was also significantly expressed in human cardiac fibroblasts. When RNA was directly amplified by PCR without reverse transcription, the bands for these positive genes disappeared (Fig. 8B), suggesting that the genes detected were not false-positive signals from genomic DNA contamination.

Discussion

In the present study, we have demonstrated that multiple ionic currents (BK_{Ca}, IK_{DR}, I_{to}, I_{Kir}, $I_{Cl.vol}$, and $I_{Na.TTX}$ and $I_{Na.TTXR}$) are present in human cardiac fibroblasts. BK_{Ca} was inhibited by paxilline, IK_{DR} and I_{to} were inhibited by 4-AP. I_{Kir} was blocked by Ba^{2+} and $I_{Cl.vol}$ was inhibited by DIDS or NPPB, while $I_{Na.TTX}$ and $I_{Na.TTXR}$ were suppressed by different concentrations of TTX. The channel genes corresponding to the functional currents (KCa1.1 for BK_{Ca}, Kv1.5/Kv1.6 for IK_{DR}, Kv4.2/Kv4.3 for I_{to}, Kir2.1/Kir2.3 for I_{Kir}, Clcn3 for $I_{Cl.vol}$, $Na_V1.2$/$Na_V1.3$/$Na_V1.6$/$Na_V1.7$ for $I_{Na.TTX}$, and $Na_V1.5$ for $I_{Na.TTXR}$) were confirmed by RT-PCR.

Recent studies demonstrated that an inward rectifier K^+ current (I_{Kir}), a delayed rectifier K^+ current (IK_{DR}), and a non-selective cation channel current were present in rat ventricular fibroblasts [11–13]. Only BK_{Ca} was described in human cardiac fibroblasts [14]. The present study provides novel information that multiple ion channels are heterogeneously expressed in human cardiac fibroblasts. In addition to BK_{Ca} as previously reported by Wang and colleagues [14], IK_{DR}, I_{to}, I_{Kir}, $I_{Cl.vol}$, $I_{Na.TTX}$, and $I_{Na.TTXR}$ were present with BK_{Ca} in different populations of human cardiac fibroblasts (Fig. 1). These currents have different distribution and properties compared to those in human cardiomyocytes [18,24–27].

Several K^+ currents have been reported in myocytes from human hearts. They include 4-AP-sensitive I_{to} (encoded by Kv1.4/Kv4.3) [28] in atrial and ventricular myocytes [18,26], 4-AP sensitive ultra-rapid delayed rectifier K^+ current (I_{Kur}, encoded by Kv1.5) in atrial myocytes [29], inward rectifier K^+ current (I_{K1}, encoded by Kir2.1/Kir2.3) [24,28,30], and rapidly and slowly-activated delayed rectifier K^+ currents (I_{Kr} and I_{Ks}) [25]. However, I_{to} (likely encoded by Kv4.2/Kv4.3) and IK_{DR} (likely encoded by Kv1.5/Kv1.6) were present only in a small population of human cardiac fibroblasts (15% and 14%, respectively) (Figs. 1–3). In addition, Ba^{2+}-sensitive inward rectifier K^+ current (likely encoded by Kir2.1/Kir2.3) with a small amplitude was present in 24% human cardiac fibroblasts, not like in human cardiomyocytes where I_{K1} is detected in each cell [24,30]. It is interesting to note

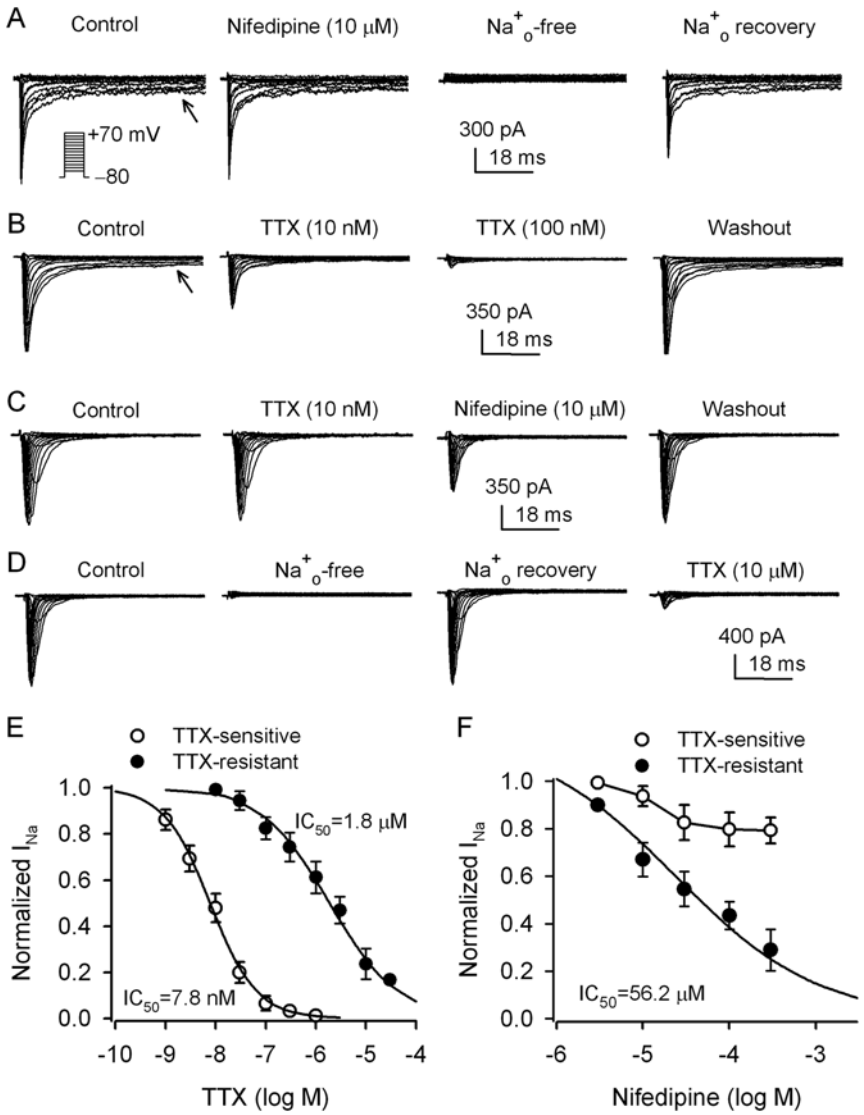

Figure 6. $I_{Na.TTX}$ and $I_{Na.TTXR}$ in human cardiac fibroblasts. ***A.*** An inward current with a persistent component (arrow) recorded in a representative cell under K^+-free conditions using the voltage steps as shown in the *inset*. Nifedipine (10 μM) had no effect on the current, while the current disappeared when Na^+_o was replaced with equimolar choline, and recovered as restoration of Na^+_o. ***B.*** Similar inward current with persistent component (arrow) recorded in another cell was highly sensitive to inhibition by low concentrations of TTX. ***C.*** An inward current with fast inactivation recorded using the same voltage protocol as shown in the *inset* of A. The current was not affected by 10 nM TTX, but reversibly inhibited by 10 μM nifedipine. ***D.*** Similar current recorded in another cell disappeared with Na^+_o removal, and recovered as restoration of Na^+_o. The current was suppressed by a high concentration of TTX (10 μM). ***E.*** Concentration-dependent response of two types of inward currents to TTX. The data were fitted to the Hill equation: $E = E_{max}/[1+(IC_{50}/C)^b]$, where E is the percentage inhibition of current at concentration C, E_{max} is the maximum inhibition, IC_{50} is the concentration for a half inhibitory effect, and b is the Hill coefficient. The IC_{50} of TTX for inhibiting TTX-sensitive I_{Na} was 7.8 nM (n = 5−9 for each concentration), the Hill coefficient was 0.94. The IC_{50} of TTX for inhibiting TTX-resistant I_{Na} was 1.8 μM (n = 6−9 cell for each concentration), the Hill coefficient was 0.58. ***F.*** Concentration-dependent relationships of $I_{Na.TTX}$ and $I_{Na.TTXR}$ to nifedipine. The IC_{50} of nifedipine for inhibiting $I_{Na.TTXR}$ was 56.2 μM (n = 4−7 cells for each concentration) with a Hill coefficient of 0.59.
doi:10.1371/journal.pone.0007307.g006

that BK_{Ca} was present in most (88%) human cardiac fibroblasts; however, this current has not been identified in human cardiomyocytes. The different distribution of K^+ currents implies the various functions of these channels in these two types of heart cells.

Earlier studies have demonstrated that $I_{Cl.vol}$ are present in human cardiac myocytes [31,32], and the current is only recorded when the hypotonic insult is applied [31,32]. Nonetheless, $I_{Cl.vol}$ is recorded in a small population (7%) of human cardiac fibroblasts without hypotonic exposure (Fig. 1), and it is activated in almost all fibroblasts with hypotonic exposure (Fig. 5). $I_{Cl.vol}$ is believed to play a role in arrhythmogenesis, myocardial injury, preconditioning, and apoptosis of myocytes [33]. Nonetheless, physiological function of $I_{Cl.vol}$ in human cardiac fibroblasts remains to be studied in the future.

It is well recognized that I_{Na} channels expressed in cardiomyocytes (mainly encoded by $Na_V1.5$) play an important role in controlling excitation-contraction and impulse conduction in the hearts. I_{Na} has been also found to participate in regulating sinus node pacemaker function [34]. In the present study, we found that I_{Na} was expressed in most (61%) human cardiac fibroblasts (Fig. 1). The $I_{Na.TTX}$ in human cardiac fibroblasts (Figs. 6 & 7) shares some properties with neuronal

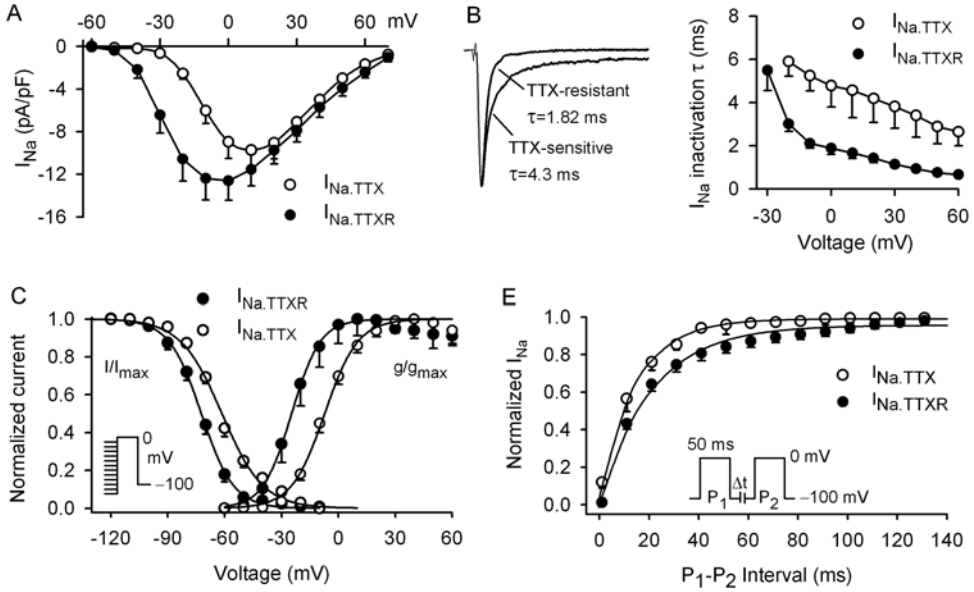

Figure 7. Kinetics of $I_{Na.TTX}$ and $I_{Na.TTXR}$. ***A.*** Mean values of *I-V* relationships of $I_{Na.TTX}$ and $I_{Na.TTXR}$. ***B.*** Left panel: inactivation time course of representative I_{Na} traces (at 0 mV) was fitted to a monoexponential function with time constant (τ) shown, 4.3 ms for $I_{Na.TTX}$ and 1.82 ms for $I_{Na.TTXR}$. Right panel: mean values of voltage dependence of inactivation of $I_{Na.TTX}$ (n = 8) and $I_{Na.TTXR}$ (n = 10). $P<0.05$ or $P<0.01$ at −20 to +60 mV. ***C.*** Voltage-dependent availability (I/I_{max}) of I_{Na} was determined with the protocol as shown in the left *inset* (with 1-s conditioning pulses from voltages between −120 and −10 mV then a 50-ms test pulse to 0 mV). Curves of I/I_{max} and activation conductance (g/g_{max}) were fitted to a Boltzmann equation. ***E.*** Recovery curves of $I_{Na.TTX}$ and $I_{Na.TTXR}$ from inactivation were fitted to a monoexponential function.
doi:10.1371/journal.pone.0007307.g007

I_{Na}, e.g. a transient inward current followed by a persistent component, sensitive to inhibition by nanomolar TTX, and likely encoded by $Na_V1.2$, $Na_V1.3$, $Na_V1.6$, and $Na_V1.7$ [35,36].

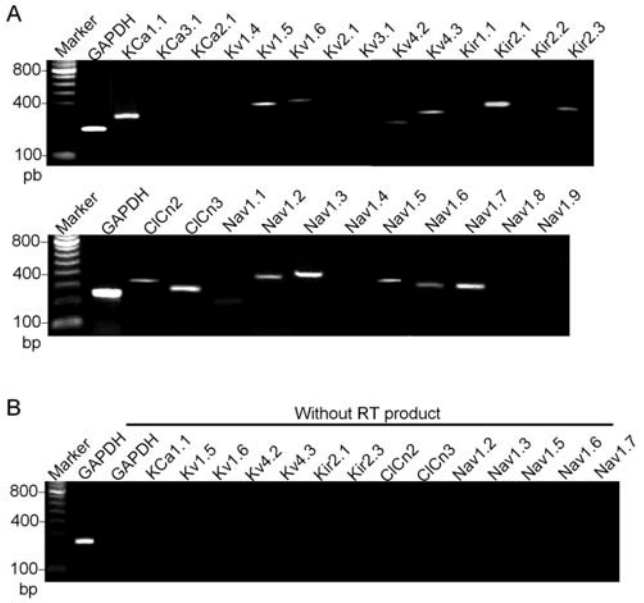

Figure 8. RT-PCR for detecting ion channels expressed in human cardiac fibroblasts. ***A.*** Images of RT-PCR products corresponding to significant gene expression of KCa1.1 (BK_{Ca}), Kv1.5 (IK_{DR}), Kv4.3 (I_{to}), and Kir2.1 (I_{Kir}) and Clcn3 ($I_{Cl.vol}$), and $Na_V1.2$, $Na_V1.3$, $Na_V1.5$, $Na_V1.6$ and $Na_V1.7$ in human cardiac fibroblasts. A weak expression of Kv4.2, Kir2.3, Clcn2 and $Na_V1.1$ was also found in human cardiac fibroblasts. ***B.*** No significant bands were observed in the PCR experiment when RT product was replaced by total RNA.
doi:10.1371/journal.pone.0007307.g008

The $I_{Na.TTXR}$ in human cardiac fibroblasts (Figs. 6 & 7) shares some features with I_{Na} in cardiomyocytes (e.g. inhibited by micromolar TTX and encoded by $Na_V1.5$) [35,37]. Some properties of $I_{Na.TTXR}$ in human cardiac fibroblasts are not identical to those of I_{Na} in human cardiomyocytes [27,37,38], e.g. more positive $V_{0.5}$s of activation (−25 mV vs −39 mV) and availability (−72 mV vs −95 mV) and more positive peak current potential (0 mV vs −35 mV), compared to I_{Na} in human cardiomyocytes [27,37]. In addition, $I_{Na.TTXR}$ in cardiac fibroblasts, as $Na_V1.5$-encoded $I_{Na.TTXR}$ in gastric epithelial cells [39], was inhibited by high concentrations of the $I_{Ca.L}$ blocker nifedipine (Fig. 6). Nonetheless, no report is available in the literature regarding the information whether I_{Na} of cardiomyocytes is sensitive to a high concentration of nifedipine. Moreover, it is unknown how $I_{Na.TTX}$ and $I_{Na.TTXR}$ participate in cellular function of cardiac fibroblasts.

It has been recognized that cardiac fibroblasts are electrically unexcitable, but they contribute to the electrophysiology of myocytes in various ways, such as electrical coupling of fibroblasts and myocytes [40]. The electrical coupling between fibroblasts and myocytes was observed at cellular and tissue level as well as in cell cultures [5,8,40–42]. Coupling between fibroblasts and myocytes was demonstrated to be via Cx43 gap junctions in sheep ventricles and Cx45 in rabbit sinoatrial node cells [4,6] and in sheep ventricular scars [43]. The cardiac fibroblasts are therefore believed to maintain electrical contact with myocytes. Our results of multiple ion channels in human cardiac fibroblasts likely provide a basis for understanding of the potential contribution of these ion channels to fibroblast-myocytes electrical coupling under physiological conditions, and also for future studies on the potential mechanism how cardiac fibroblasts participate in regulating cardiac electrophysiology.

In proliferative cells, ion channels play a role in cell cycle progression [44,45]. The activity of BK_{Ca} (i.e. KCa1.1) channels was regulated by the spontaneous Ca^{2+} oscillations, resulting in

fluctuations of membrane currents and potentials. BK_{Ca} was reported to play a role in regulating proliferation of human preadipocytes [46], endothelial cells [47], and breast cancer cells [48]. I_{Kir} was found to participate in regulating the proliferation of human hematopoietic progenitor cells [49]. Although the underlying mechanisms of ion channels in cell proliferation regulation remain elusive, the involvement of K^+ channels in cell proliferation was well established [44,45,49]. Further exploration is required to find out whether these ion channels contribute to human cardiac fibroblast proliferation.

Clcn3 channel is regarded as one of the candidate channels for volume regulated anion channels and has been shown to play an important role in cell proliferation and apoptosis [45]. Blockade or disruption of Clcn3 channel resulted in arrest of cell cycle and prevention of cell proliferation in several cell types [21,50]. The present observation demonstrated that functional chloride current encoded by Clcn3, sensitive to cell volume, was observed in human cardiac fibroblasts (Fig. 5). Whether this I_{Cl} current would contribute to human cardiac fibroblast proliferation remains to be studied in the future.

One of limitations of the present study was that ion channels, BK_{Ca}, I_{to}, I_{Kir} and $I_{Cl.vol}$, and $I_{Na.TTX}$, and $I_{Na.TTXR}$, were heterogeneously expressed within the same species of cultured human cardiac fibroblasts. This could result from heterogeneous cell population of the fibroblasts. An earlier study demonstrated that myofibroblast could differentiate from fibroblasts when plated at low density and could revert back to fibroblasts at higher density [51]. Consequently, a subpopulation of human cardiac fibroblasts may display different patterns of ion channel expression.

In summary, the present study provides the first information that multiple ion channel currents are present in cultured human cardiac fibroblasts, the patterns and properties of these ion channel currents differ from those observed in human cardiac myocytes. The information obtained form the present study provides a basis for future study how ion channels participate in regulating cardiac electrophysiology.

Acknowledgments

The authors thank Mr. Wentao Li for reading the manuscript, and Ms Xiao-Hua Zhang for performing part of experiments.

Author Contributions

Conceived and designed the experiments: GRL HFT CPL. Performed the experiments: HYS JBC YZ. Analyzed the data: GRL HYS. Wrote the paper: GRL.

References

1. Camelliti P, Green CR, Kohl P (2006) Structural and functional coupling of cardiac myocytes and fibroblasts. Adv Cardiol 42: 132–149.
2. Brown RD, Ambler SK, Mitchell MD, Long CS (2005) The cardiac fibroblast: therapeutic target in myocardial remodeling and failure. Annu Rev Pharmacol Toxicol 45: 657–687.
3. Flack EC, Lindsey ML, Squires CE, Kaplan BS, Stroud RE, et al. (2006) Alterations in cultured myocardial fibroblast function following the development of left ventricular failure. J Mol Cell Cardiol 40: 474–483.
4. Camelliti P, Green CR, LeGrice I, Kohl P (2004) Fibroblast network in rabbit sinoatrial node: structural and functional identification of homogeneous and heterogeneous cell coupling. Circ Res 94: 828–835.
5. Gaudesius G, Miragoli M, Thomas SP, Rohr S (2003) Coupling of cardiac electrical activity over extended distances by fibroblasts of cardiac origin. Circ Res 93: 421–428.
6. Kohl P, Camelliti P, Burton FL, Smith GL (2005) Electrical coupling of fibroblasts and myocytes: relevance for cardiac propagation. J Electrocardiol 38: 45–50.
7. Miragoli M, Gaudesius G, Rohr S (2006) Electrotonic modulation of cardiac impulse conduction by myofibroblasts. Circ Res 98: 801–810.
8. Rook MB, van Ginneken AC, de Jonge B, el Aoumari A, Gros D, et al. (1992) Differences in gap junction channels between cardiac myocytes, fibroblasts, and heterologous pairs. Am J Physiol 263: C959–C977.
9. Kohl P (2003) Heterogeneous cell coupling in the heart: an electrophysiological role for fibroblasts. Circ Res 93: 381–383.
10. Kohl P, Camelliti P (2007) Cardiac myocyte-nonmyocyte electrotonic coupling: implications for ventricular arrhythmogenesis. Heart Rhythm 4: 233–235.
11. Chilton L, Ohya S, Freed D, George E, Drobic V, et al. (2005) K^+ currents regulate the resting membrane potential, proliferation, and contractile responses in ventricular fibroblasts and myofibroblasts. Am J Physiol Heart Circ Physiol 288: H2931–H2939.
12. Shibukawa Y, Chilton EL, Maccannell KA, Clark RB, Giles WR (2005) K^+ currents activated by depolarization in cardiac fibroblasts. Biophys J 88: 3924–3935.
13. Rose RA, Hatano N, Ohya S, Imaizumi Y, Giles WR (2007) C-type natriuretic peptide activates a non-selective cation current in acutely isolated rat cardiac fibroblasts via natriuretic peptide C receptor-mediated signalling. J Physiol 580: 255–274.
14. Wang YJ, Sung RJ, Lin MW, Wu SN (2006) Contribution of BK(Ca)-channel activity in human cardiac fibroblasts to electrical coupling of cardiomyocytes-fibroblasts. J Membr Biol 213: 175–185.
15. Li GR, Sun H, Deng X, Lau CP (2005) Characterization of ionic currents in human mesenchymal stem cells from bone marrow. Stem Cells 23: 371–382.
16. Li GR, Deng XL, Sun H, Chung SS, Tse HF, et al. (2006) Ion channels in mesenchymal stem cells from rat bone marrow. Stem Cells 24: 1519–1528.
17. Gao Z, Sun HY, Lau CP, Chin-Wan FP, Li GR (2007) Evidence for cystic fibrosis transmembrane conductance regulator chloride current in swine ventricular myocytes. J Mol Cell Cardiol 42: 98–105.
18. Li GR, Feng J, Wang Z, Fermini B, Nattel S (1995) Comparative mechanisms of 4-aminopyridine-resistant Ito in human and rabbit atrial myocytes. Am J Physiol 269: H463–H472.
19. Gao Z, Sun H, Chiu SW, Lau CP, Li GR (2005) Effects of diltiazem and nifedipine on transient outward and ultra-rapid delayed rectifier potassium currents in human atrial myocytes. Br J Pharmacol 144: 595–604.
20. Li GR, Sun H, Nattel S (1998) Characterization of a transient outward K^+ current with inward rectification in canine ventricular myocytes. Am J Physiol 274: C577–C585.
21. Tao R, Lau CP, Tse HF, Li GR (2008) Regulation of cell proliferation by intermediate-conductance Ca^{2+}-activated potassium and volume-sensitive chloride channels in mouse mesenchymal stem cells. Am J Physiol Cell Physiol 295: C1409–C1416.
22. Li GR, Yang B, Feng J, Bosch RF, Carrier M, et al. (1999) Transmembrane I_{Ca} contributes to rate-dependent changes of action potentials in human ventricular myocytes. Am J Physiol 276: H98–H106.
23. Liu H, Sun HY, Lau CP, Li GR (2007) Regulation of voltage-gated cardiac sodium current by epidermal growth factor receptor kinase in guinea pig ventricular myocytes. J Mol Cell Cardiol 42: 760–768.
24. Li GR, Lau CP, Leung TK, Nattel S (2004) Ionic current abnormalities associated with prolonged action potentials in cardiomyocytes from diseased human right ventricles. Heart Rhythm 1: 460–468.
25. Li GR, Feng J, Yue L, Carrier M, Nattel S (1996) Evidence for two components of delayed rectifier K^+ current in human ventricular myocytes. Circ Res 78: 689–696.
26. Li GR, Feng J, Yue L, Carrier M (1998) Transmural heterogeneity of action potentials and Ito1 in myocytes isolated from the human right ventricle. Am J Physiol 275: H369–H377.
27. Feng J, Li GR, Fermini B, Nattel S (1996) Properties of sodium and potassium currents of cultured adult human atrial myocytes. Am J Physiol 270: H1676–H1686.
28. Gaborit N, Le Bouter S, Szuts V, Varro A, Escande D, et al. (2007) Regional and tissue specific transcript signatures of ion channel genes in the non-diseased human heart. J Physiol 582: 675–693.
29. Fedida D, Wible B, Wang Z, Fermini B, Faust F, et al. (1993) Identity of a novel delayed rectifier current from human heart with a cloned K^+ channel current. Circ Res 73: 210–216.
30. Beuckelmann DJ, Nabauer M, Erdmann E (1993) Alterations of K^+ currents in isolated human ventricular myocytes from patients with terminal heart failure. Circ Res 73: 379–385.
31. Du XL, Gao Z, Lau CP, Chiu SW, Tse HF, et al. (2004) Differential effects of tyrosine kinase inhibitors on volume-sensitive chloride current in human atrial myocytes: evidence for dual regulation by Src and EGFR kinases. J Gen Physiol 123: 427–439.
32. Li GR, Feng J, Wang Z, Nattel S (1996) Transmembrane chloride currents in human atrial myocytes. Am J Physiol 270: C500–C507.
33. Baumgarten CM, Clemo HF (2003) Swelling-activated chloride channels in cardiac physiology and pathophysiology. Prog Biophys Mol Biol 82: 25–42.
34. Lei M, Zhang H, Grace AA, Huang CL (2007) SCN5A and sinoatrial node pacemaker function. Cardiovasc Res 74: 356–365.
35. Goldin AL (2001) Resurgence of sodium channel research. Annu Rev Physiol 63: 871–894.
36. Hammarstrom AK, Gage PW (1999) Nitric oxide increases persistent sodium current in rat hippocampal neurons. J Physiol 520 Pt 2: 451–461.

37. Sakakibara Y, Wasserstrom JA, Furukawa T, Jia H, Arentzen CE, et al. (1992) Characterization of the sodium current in single human atrial myocytes. Circ Res 71: 535–546.
38. Furukawa T, Koumi S, Sakakibara Y, Singer DH, Jia H, et al. (1995) An analysis of lidocaine block of sodium current in isolated human atrial and ventricular myocytes. J Mol Cell Cardiol 27: 831–846.
39. Wu WK, Li GR, Wong HP, Hui MK, Tai EK, et al. (2006) Involvement of Kv1.1 and Nav1.5 in proliferation of gastric epithelial cells. J Cell Physiol 207: 437–444.
40. Sachse FB, Moreno AP, Abildskov JA (2008) Electrophysiological modeling of fibroblasts and their interaction with myocytes. Ann Biomed Eng 36: 41–56.
41. Camelliti P, McCulloch AD, Kohl P (2005) Microstructured cocultures of cardiac myocytes and fibroblasts: a two-dimensional in vitro model of cardiac tissue. Microsc Microanal 11: 249–259.
42. Kohl P, Kamkin AG, Kiseleva IS, Noble D (1994) Mechanosensitive fibroblasts in the sino-atrial node region of rat heart: interaction with cardiomyocytes and possible role. Exp Physiol 79: 943–956.
43. Camelliti P, Devlin GP, Matthews KG, Kohl P, Green CR (2004) Spatially and temporally distinct expression of fibroblast connexins after sheep ventricular infarction. Cardiovasc Res 62: 415–425.
44. Pardo LA (2004) Voltage-gated potassium channels in cell proliferation. Physiology (Bethesda) 19: 285–292.
45. Nilius B (2001) Chloride channels go cell cycling. J Physiol 532: 581.
46. Hu H, He ML, Tao R, Sun HY, Hu R, et al. (2008) Characterization of ion channels in human preadipocytes. J Cell Physiol 218: 427–435.
47. Kuhlmann CR, Most AK, Li F, Munz BM, Schaefer CA, et al. (2005) Endothelin-1-induced proliferation of human endothelial cells depends on activation of K^+ channels and Ca^{2+} influx. Acta Physiol Scand 183: 161–169.
48. Coiret G, Borowiec AS, Mariot P, Ouadid-Ahidouch H, Matifat F (2007) The antiestrogen tamoxifen activates BK channels and stimulates proliferation of MCF-7 breast cancer cells. Mol Pharmacol 71: 843–851.
49. Shirihai O, Attali B, Dagan D, Merchav S (1998) Expression of two inward rectifier potassium channels is essential for differentiation of primitive human hematopoietic progenitor cells. Journal Of Cellular Physiology 177: 197–205.
50. Wang GL, Wang XR, Lin MJ, He H, Lan XJ, et al. (2002) Deficiency in ClC-3 Chloride Channels Prevents Rat Aortic Smooth Muscle Cell Proliferation. Circ Res 91: 28e–32.
51. Masur SK, Dewal HS, Dinh TT, Erenburg I, Petridou S (1996) Myofibroblasts differentiate from fibroblasts when plated at low density. Proc Natl Acad Sci U S A 93: 4219–4223.